Dimerization and α-Cyclodextrin Inclusion of Propantheline Bromide as Studied by NMR and Molecular Modeling

Sakae Hada, Seiji Ishikawa, Saburo Neya, and Noriaki Funasaki*

Kyoto Pharmaceutical University, Misasagi, Yamashina-ku, Kyoto 607-8414, Japan

Received: September 28, 1998

The proton chemical shifts of propantheline bromide (PB) and α-cyclodextrin (α-CyD) are determined as a function of the PB concentration in the absence and presence of 5 mmol dm^{-3} α-CyD. The dimerization constant and the critical micelle concentration of PB are determined to be 20 dm^3 mol^{-1} and 18 mmol dm^{-3}. The chemical shift variations of PB protons induced with the dimerization of PB agree very well with the values calculated on the basis of the antiparallel stacking of two xanthene rings. The 1:1 binding constant and the chemical shifts of PB and α-CyD protons for their complex are evaluated from the concentration dependence of the chemical shifts. On the basis of both these shift data and molecular mechanical calculations, it is estimated that one of the benzene rings of PB in the complex is included shallowly from the wider side into the α-CyD cavity. The chemical shifts of the α-CyD protons, calculated on the basis of the effect of the xanthene ring current for this structure, agree excellently with the observed ones.

Introduction

Recently, we have investigated the self-association pattern of the antiacetylcholine drug, propantheline bromide (PB), by gel filtration chromatography. PB self-associates stepwise to form dimer and larger multimers.[1] Although PB is a bitter drug, its bitterness is depressed by the addition of α-, *β*-, and *γ*-cyclodextrin (CyD). Their binding constants were determined by the surface tension method and UV spectroscopy. The suppression of the bitter taste intensity was predicted by the surface tension method. Furthermore, the structures of some complexes of PB with α-, *β*-, and *γ*-CyD were proposed on the basis of their molecular size and the affinity of their atomic groups.[2]

In aqueous media, the self-association and CyD inclusion of many drugs are controlled by hydrophobic interactions. Their aggregates are formed by the stacking of aromatic rings in most cases.[3−6] The solution structures of CyD inclusion complexes are estimated by NMR spectroscopy, circular dichroism, and molecular modeling. However, the estimated structures are rather rough in most cases.[7−13] Johnson and Bovey proposed the theory which estimates the magnitude of the shielding effect of the benzene molecule on the chemical shift of a proton.[14] Yamamoto et al. applied this theory to determine the solution structures of the equimolar complexes of 4-nitrophenol with CyDs.[8]

In the present work we determine the dimerization constant of PB from the concentration dependence of the chemical shift of a PB proton and estimate the solution structure of the PB dimer on the basis of the Johnson-Bovey theory and molecular modeling. Furthermore, we determine the 1:1 binding constant of PB and α-CyD from the variations of chemical shifts of the H3 proton of α-CyD with the concentration of PB and estimate the solution structure of its 1:1 complex from the variations of chemical shift of the α-CyD protons on the basis of the Johnson-Bovey theory and molecular modeling. From its estimated solution structure, we suggest that the complex is more hydrophilic and less bitter than the PB molecule alone.

* Corresponding author. Fax: +81-75-595-4762. E-mail: funasaki@mb.kyoto-phu.ac.jp.

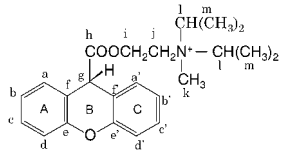

Figure 1. Labeling of the carbon atoms of PB.

Experimental Section

Materials. Commercial samples of α-CyD (Nacalai Tesque, Kyoto), 99% deuterium hydroxide (Aldrich), and PB (Sigma) were used as received.

NMR Measurements. All NMR experiments were carried out in deuterium oxide at 309.7 K. NMR spectra were obtained with a JEOL Lambda 500 spectrometer. Chemical shifts were referenced to the internal water signal at 4.65 ppm. The chemical shifts of the PB protons and the α-CyD protons were determined as a function of the PB concentration in the absence and presence of 5 mmol dm^{-3} α-CyD. The $^1H-^1H$ shift correlated spectrum ($^1H-^1H$ COSY) of a 40 mmol dm^{-3} PB solution was obtained with the JEOL standard pulse sequences. The data processing was performed with a JEOL standard software.

Molecular Modeling. Molecular mechanical calculations of the complex were performed with the Biosym Insight II/Discover (95.0) on a Silicon Graphics Indigo 2 workstation. The Discover CVFF force field was used for energy minimization. All calculations were performed in the presence of water. The starting structure of the PB molecule (Figure 1) for the structure of PB-α-CyD complex was generated by the manual-drawing routine in Insight II. The counterion of PB was neglected. The partial atomic charges and the structure of PB in vacuo were obtained by optimization using AMPAC/MOPAC module of Insight II with PM3 and potential types were derived from the CVFF force field. The optimized structure of PB was then soaked in a 1 nm layer of water and then its total conformational energy was minimized.

The starting structure of α-cyclodextrin molecule was the published coordinates of the X-ray crystal structure of α-CyD−$6H_2O$.[15] This structure was then soaked in a 2 nm layer of water

10.1021/jp983873c CCC: $18.00
Published on Web 03/12/1999

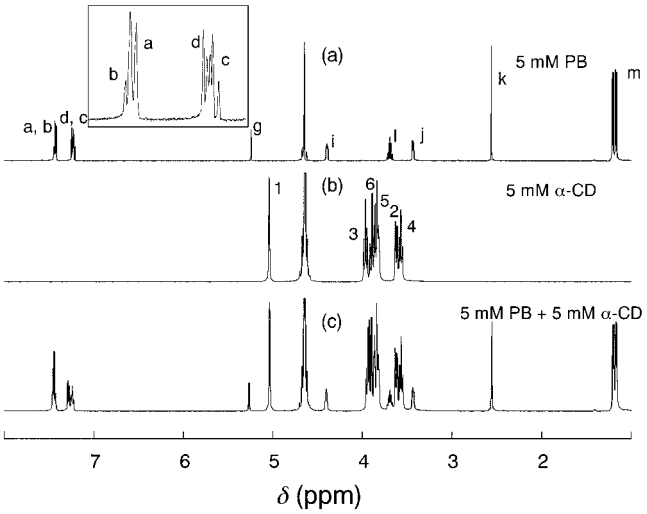

Figure 2. 500 MHz ^{1}H NMR spectra of deuterium oxide solutions of (a) 5.0 mmol dm^{-3} PB, (b) 5.0 mmol dm^{-3} α-CyD, and (c) 5.0 mmol dm^{-3} PB +5.0 mmol dm^{-3} α-CyD at 309 K.

and minimized the total conformational energy. This minimization produced little changes in the structure. Energy minimization was performed using the conjugate gradients method to a derivative of 0.001 kcal mol^{-1} with Insight II′ default values (VDW cut off distance = 0.95 nm and electrostatic cut off distance = 0.95 nm).

Docking experiments were performed to position the PB molecule in the cavity at the wider, secondary hydroxyl side of the α-CyD molecule, while the structures of these respective molecules were kept rigid. Because the xanthene ring of PB is too large to be totally incorporated in the cavity of α-CyD, only one of the benzene rings of xanthene penetrated therein. Then this complex was soaked in a 2 nm layer of water, and the total potential energy of the complex was minimized for the determination of its stable structure.

Results

Self-Association of Propantheline Bromide. A 500 MHz ^{1}H NMR spectrum of PB in deuterium oxide is shown in Figure 2a. The assignments of the PB protons are included therein. The assignments of the side chain were carried out in reference to those in the 90 and 400 MHz spectra.[16,17] The Hb proton and the Hc proton appear to be the triplets owing to the vicinal spin−spin coupling with the Ha and Hc protons and the Hd and Hb protons, respectively. The Ha and Hd protons appear to be boublet owing to the vicinal spin−spin coupling with the Hb and Hc protons, respectively. As Figure 2a shows, two pairs of a doublet and a triplet are overlapped around 7.2 and 7.1 ppm, respectively. As the PB concentration is increased, all peaks of these protons are separated. In the ^{1}H−^{1}H COSY spectrum of a 40 mmol dm^{-3} PB solution, the doublet indicating a long-range coupling with the Hg proton was assigned to the Ha proton. This allows us to assign the doublet of the Hd proton and the triplets of the Hb and Hc protons and to determine the vicinal coupling constants of $^3J_{HaHb}$, $^3J_{HbHc}$, and $^3J_{HcHd}$. Using these ^3J values, we could determine the chemical shifts of all aromatic protons of PB as a function of the PB concentration.

We determined the concentration dependence of chemical shifts of the PB protons up to 100 mmol dm^{-3} PB. All PB protons exhibit high-field shifts with the increasing PB concentration, namely, negative δ (chemical shift) values (Table 1). The chemical shift of the Hg proton, which exhibits the largest change among all PB protons, is plotted against the reciprocal of PB concentration in Figure 3. Assuming that two straight lines approximate this relation, we obtained a critical micelle concentration (cmc) of 18 mmol dm^{-3} from the intersection of these lines. Close cmc values were obtained from analysis of chemical shifts of other PB protons, and these cmc values are larger than those determined in a 154 mmol dm^{-3} NaBr solution by the surface tension method.[2] This difference in cmc is explicable on the basis of electrostatic effects of the salt. PB self-associates stepwise to form dimer and higher multimers.[1] Figure 4 illustrates the concentration dependence of the changes in chemical shifts of the xanthene ring protons. The chemical shifts of the side chain protons exhibit a similar concentration dependence and overlap with those of other protons.

On the basis of our investigations of the self-association of drugs, we can presume, without significant errors, that PB forms

TABLE 1: Observed[a] and Calculated Chemical Shift Variations of PB Protons with Dimerization and Observed Variations with α-CyD Inclusion

	δ_{P1}(ppm)	$\Delta\delta_{P2}$(ppm)			$\Delta\delta_{PPD}$(ppm)
			calcd		
	obsd	obsd	structure **A**	structure **B**	obsd
Ha	7.4620	−0.202	−0.154	−0.168	0.046
Hb	7.4480	−0.089	−0.218	−0.045	0.019
Hc	7.2362	−0.078	−0.116	−0.051	0.065
Hd	7.2610	−0.156	−0.072	−0.126	0.209
Hg	5.2875	−0.348	−0.215	−0.356	0.091
Hi	4.4110	−0.121	−0.046	−0.053	0.045
Hj	3.4482	−0.123	−0.035	−0.048	0.005
Hk	2.5679	−0.085	−0.026	−0.030	−0.005
Hl	3.7047	−0.090	−0.018	−0.020	−0.006
Hm	1.1962	−0.077	−0.012	−0.007	−0.007
SS			0.0714	0.0279	

[a] obsd = observed.

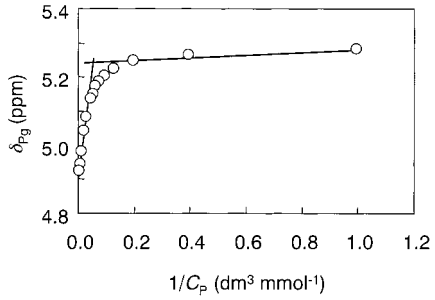

Figure 3. Plots of chemical shifts of PB proton g against the reciprocal concentration of PB. The intersection of two straight lines gives a cmc of 18 mmol dm^{-3}.

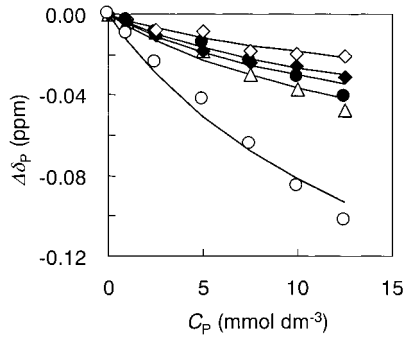

Figure 4. Concentration dependence of chemical shift variations for the xanthene ring protons of 5.0 mmol dm^{-3} PB (Ha, ●; Hb, ■; Hc, □; Hd, △; Hg; ○) on the addition of 5.0 mmol dm^{-3} α-CyD. The solid lines show theoretical shifts calculated from eq 1 using values of k_2 = 20 dm^3 mol^{-1} and $\Delta\delta_{P2}$ shown in Table 1.

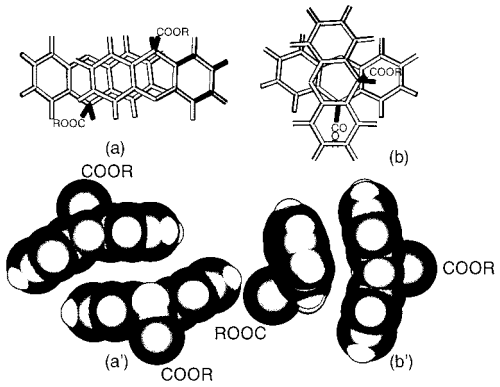

Figure 5. Two possible structures of PB dimer: (a) and (a′) parallel stacking **A** and (b and b′) perpendicular structure **B**. Views a′ and b′ are different projections of (a and b).

dimer alone below ca. 15 mmol dm^{-3}.[1,4] When the dimerization constant of PB is denoted by k_2, the observed chemical shift δ_P of a PB proton can be written as

$$\delta_P = (\delta_{P1}[P] + 2\delta_{P2}[P_2])/C_P$$
$$= (\delta_{P1}[P] + 2\delta_{P2}k_2[P]^2)/C_P \quad (1)$$

Here δ_{P1} and δ_{P2} denote the chemical shifts of monomer and dimer of PB, P and P_2 stand for monomer and dimer, and C_P is the total concentration of PB. The monomer chemical shift δ_{P1} was obtained by the extrapolation of observed values in dilute solutions to infinite dilution. Because the concentration dependence of the Hg proton is the greatest among those of all protons, we determined values of $k_2 = 20$ dm^3 mol^{-1} and $\Delta\delta_{P2} = -0.36$ ppm by best fitting eq 1 to the observed shifts of this proton. Next, we determined values of δ_{P2} for the other protons of PB by best fitting eq 1 to the observed shifts, using a value of $k_2 = 20$ dm^3 mol^{-1}. These δ_{P2} values are shown in the form of $\Delta\delta_{P2} = \delta_{P2} - \delta_{P1}$ in Table 1. The solid lines in Figure 4 show the best fit values.

Structure of Dimer of PB. The chemical shift changes with dimerization, shown in Table 1, allow us to estimate the three-dimensional structure of dimer. These changes will be ascribed mainly to the proximity of xanthene ring of the other PB molecule due to dimerization: this proximity will cause some shifts due to the ring-current effect of the xanthene group.

First, we estimated the structure of PB monomer in water from molecular−mechanical calculations using the Discover CVFF force field in the presence of water. This nonplanar, folded structure is shown in Figure 5, where the structure of the side chain is not shown for simplicity and uncertainty. The xanthene ring has the structure in which the A and C benzene rings fold at the line connecting two atoms O and Cg of the central ring B (Figure 1). This energy-optimized structure of the xanthene ring agrees with that derived from polarity and polarizability data in CCl_4 and benzene.[18] This structure of the xanthene ring is also close to that in the crystal structure of xanthene 9−carboxylic acid,[19] albeit slightly less folded.

Keeping this energy-minimized structure of monomer rigid, we constructed two structures **A** and **B** for the dimer of PB using the Discover docking tool. These dimer structures **A** and **B** were not fully energy-minimized: in particular, the distance between monomers 1 and 2 is not refined in detail. Two views of the dimer structure **A** are shown in a and a′ of Figure 5. Here the A_1 and B_1 rings of monomer 1 face parallel to the B_2 and A_2 rings of monomer 2 and the charged ammonium groups lie along opposite, owing to minimizing electrostatic repulsion between them. In the dimer structure **B** shown in b and b′ of Figure 5, the B rings of two monomers stack vertically to one another.

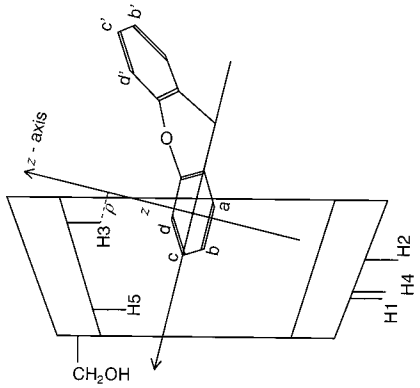

Figure 6. Definition of cylindrical z and ρ coordinates for calculations of the chemical shifts of α-CyD protons induced by the ring current effect. The origin centered on the benzene ring. The z and ρ coordinates of the H3 proton are demonstrated by the dashed lines.

For these dimer structures we calculated shifts induced by the ring-current effect using the Johnson−Bovey table for benzene.[14] The shift induced by the ring current effect of benzene is given as a function of the z and ρ coordinates in the cylindrical polar coordinate system having the origin at the center of the benzene ring (Figure 6). These coordinates are transformed to z and $(x^2 + y^2)^{1/2}$ in the Cartesian coordinate system, respectively. Thus, the ring current induced shift is independent of the direction on the $x-y$ plane. In the dimer of PB, the chemical shift of each proton of monomer 1 is influenced by the benzene rings A and C of monomer 2. We assumed the additivity of these effects. For instance, the Ha proton of ring A_1 of monomer 1 is magnetically influenced with their dimerization by benzene rings A_2 and C_2 of monomer 2. By calculating the z and ρ coordinates for ring A_2, we read the corresponding shift value from the Johnson-Bovey table and further read the shift value due to ring C_2. The sum of these shifts is the shift of the Ha proton with dimerization. Because the Ha′ proton of ring C_1 of monomer 1 is magnetically equivalent with Ha proton of ring A_1, we calculate the shift of this proton induced by dimerization. Their average is the theoretical change in $\Delta\delta$ for protons Ha and Ha′. The same calculation was carried out for the protons of monomer 2. The theoretical change for protons Ha and Ha′ is the average of the changes induced by monomers 1 and 2. As the fourth and fifth rows (labeled Ha) of Table 1 show, this theoretical value depends on the dimer structures **A** and **B**. The theoretical values for the other protons, calculated in a similar way, are included in Table 1.

For both the two dimer structures, we searched the best fit intermolecular distance (at an interval of 0.01 nm) on the basis of chemical shift variations. The best fitting was judged from the magnitude of the SS value:

$$SS = \sum_n (\delta_{obsd} - \delta_{calcd})^2 \quad (2)$$

Here n denotes the number of data. We used the nine protons of PB ($n = 9$) shown in Table 1. The intermolecular distance was optimized for structures **A** and **B**. As the SS values in Table 1 show, structure **B** is better than structure **A**. Thus, the dimer of PB has the three-dimensional structure **B** in which the central rings of two PB molecules stack vertically to one another.

Inclusion of PB by α-CyD. Figure 2b shows the 500 MHz proton NMR spectrum of a 5 mmol dm^{-3} α-CyD solution. The

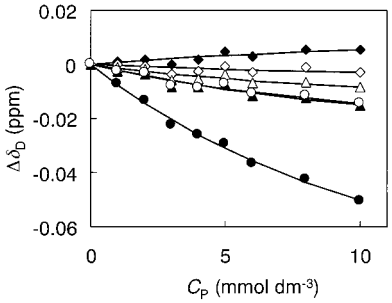

Figure 7. Changes in chemical shifts of α-CyD (5.0 mmol dm^{-3}) protons (H1, ○; H2, △; H3, ●; H4, ▲; H5, □; H6; ■) with increasing PB concentration. The solid lines are calculated using a value of K_1 = 61 dm^3 mol^{-1} and the observed values of δ_{DPD} shown in Table 2.

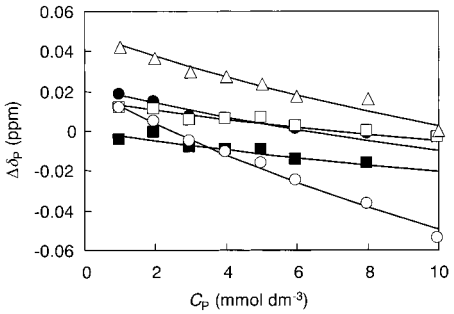

Figure 8. Changes in chemical shift of each proton of PB (Ha, ●; Hb, ■; Hc, □; Hd, △; Hg, ○) from δ_{P1} with increasing PB concentration in the presence of 5 mmol dm^{-3} CyD. The solid lines are calculated using values of K_1 = 61 dm^3 mol^{-1}, k_2 = 20 dm^3 mol^{-1}, and the observed values of $\Delta\delta_{P2}$ and $\Delta\delta_{PPD}$ shown in Table 1.

assignment of each proton of α-CyD has been established in the literature.[20] Figure 2c shows the spectrum of a solution containing 5 mmol dm^{-3} PB and 5 mmol dm^{-3} α-CyD. Figure 7 shows the change, $\Delta\delta_D$, in chemical shift of the CyD proton in a 5 mmol dm^{-3} α-CyD solution with the addition of PB. The H6 protons of α-CyD shift to a lower field, whereas the other CyD protons shift to a higher field. These changes result from the inclusion of PB in the cavity of α-CyD. Figure 8 shows the change, $\Delta\delta_P$, in chemical shift of the PB proton as a function of PB concentration in the presence of 5 mmol dm^{-3} α-CyD.

To analyze these chemical shift data, we assumed the 1:1 complexation of PB (P) and α-CyD (D), as have already been reported.[2] When its equilibrium binding constant is denoted by K_1, we can express the chemical shift of an α-CyD proton, δ_D, as

$$\delta_D = ([D]\delta_{D1} + [PD]\delta_{DPD})/C_D$$
$$= ([D]\delta_{D1} + K_1[P][D]\delta_{DPD})/C_D \quad (3)$$

Here δ_{D1} and δ_{DPD} are chemical shifts of the α-CyD protons in the free state and the 1:1 complex, respectively.

Because the chemical shift δ_P of a PB proton can be represented by the sum of fractional contributions from the monomeric, dimeric, and complexed PB molecules, we can write it as

$$\delta_P = ([P]\delta_{P1} + 2k_2[P]^2\delta_{P2} + K_1[P][D]\delta_{PPD})/C_P \quad (4)$$

Here δ_{PPD} is chemical shift of the PB proton in the complex. The total concentrations of α-CyD and PB are expressed as

$$C_D = [D] + K_1[P][D] \quad (5)$$

$$C_P = [P] + 2k_2[P]^2 + K_1[P][D] \quad (6)$$

As eq 4 shows, the chemical shift of the PB proton changes with the dimerization and α-CyD inclusion of PB (Figure 8). On the other hand, as eq 3 shows, the chemical shift of the α-CyD proton changes with the inclusion of PB alone. The chemical shift of the H3 proton exhibits the largest change among the α-CyD protons. Thus, we used the chemical shift of this proton to determine the 1:1 binding constant. As δ_{D1} we employed the observed chemical shift of the H3 proton at C_D = 5 mmol dm^{-3} in eq 3 and used a dimerization constant of 20 dm^3 mol^{-1}. We calculated the free concentrations of PB and α-CyD from eqs 5 and 6 at a given set of C_P and C_D = 5 mmol dm^{-3}, regarding K_1 and δ_{DPD} for the H3 proton as adjustable parameters. We determined best fit values of K_1 = 61 dm^3 mol^{-1} and δ_{DPD} = −0.17 ppm by a nonlinear least-squares method. Using this K_1 value, we determined the best fit values δ_{DPD} for the other α-CyD protons. These values for the complexed α-CyD protons are summarized in Table 2. Next, using eqs 4−6 with the estimated δ_{P1} and δ_{P2} values and K_1 = 61 dm^3 mol^{-1}, we determined the best-fit values of δ_{PPD} for all PB protons in the complex, as shown in Table 1. All $\Delta\delta_{PPD}$ values of PB except for the Hm protons are positive. The solid lines in Figures 7 and 8 show the values calculated from the above theory. The chemical shifts of the CyD protons are changed to a lower or higher field by the inclusion of PB, whereas those of the PB protons are decreased by both the dedimerization and inclusion of PB. The present K_1 value is close to a value of 80 dm^3 mol^{-1} obtained in a 154 mmol dm^{-3} sodium bromide solution at 309.7 K by the surface tension method.[2]

TABLE 2: Observed[a] and Calculated Values for Chemical Shift Variations of the α-CyD Protons with the 1:1 Complexation of PB and α-CyD

			$\Delta\delta_{DPDcalcd}$(ppm)	
	δ_{D1} (ppm)	$\Delta\delta_{DPDobsd}$ (ppm)	structure **A**	structure **B**
H1	5.0476	−0.049	−0.027	−0.042
H2	3.6282	−0.029	−0.040	−0.048
H3	3.9727	−0.172	−0.172	−0.193
H4	3.5773	−0.051	−0.026	−0.045
H5	3.8275	−0.010	0.071	−0.011
H6	3.8977	0.018	0.058	0.018
SS			0.0094	0.0027

[a] obsd = observed.

Structure of the 1:1 Complex of PB and α-CyD. The changes in chemical shift with the 1:1 complexation, shown in Tables 1 (PB protons) and 2 (CyD protons), allow us to estimate the three-dimensional structure of the 1:1 complex. In particular, those of the α-CyD protons will result exclusively from the ring current effect of PB. As Table 2 shows, the change in chemical shift of the H3 proton is largest among all protons of α-CyD. This proton is located inside the cavity and near the wider opening rim of the cavity (Figure 6). This result indicates that the PB molecule penetrates the cavity from the side of the wider opening (the side of the secondary alcohols of α-CyD).

Keeping this result in mind, we sought the most stable structure of the complex with a Discover docking tool. First, we energy-optimized the structure of α-CyD in the presence of water by using the crystal structures of α-CyD·6H_2O as an initial structure.[15] The structure of the side chain of PB is uncertain, because it has many freely rotating single bonds. Keeping these structures of PB and α-CyD rigid, we docked a PB molecule into the cavity of α-CyD from the wider opening side and

Figure 9. Cross sections of structures **A** and **B** for the α-CyD/PB inclusion complex.

searched more stable structures by automatically changing the depth of penetration and orientation of the PB molecule in the α-CyD cavity. The stability of the complex was judged from the magnitude of the potential energy that is composed of Coulombic and van der Waals energies. The final structure of the complex is structure **A** shown in Figure 9.

On the basis of this structure, we calculated the chemical shifts of the α-CyD protons induced by the ring current effect of the PB molecule. Figure 6 sketches the structure of the complex, shown in Figure 9, for brevity. For instance, the chemical shift of the H3 proton is calculated as follows. The chemical shift of one of the six H3 protons in the α-CyD molecule is influenced by the ring current effect of the PB molecule. First, we determined the z and ρ coordinates of the CyD protons in the cylindrical polar coordinate system having the origin at the center of the ring A (Figure 6) and then read the shift value corresponding to these coordinates from the Johnson−Bovey table.[14] This process is repeated for the benzene ring C to determine the theoretical shift induced by this ring. The summation of them is the theoretical shift of this specific H3 proton. The above process is repeated for the other five H3 protons. The average of the six H3 protons is the theoretical shift of the H3 proton, which is shown in the form of $\Delta\delta_{DPDcalc}$ in Table 2. The theoretical values of the other five kinds of the α-CyD protons are also included in this table. These theoretical $\Delta\delta_{DPD}$ values agree rather well with the observed ones.

Furthermore, we searched a better structure. In structure **A**, the side chain of PB in van der Waals contact with the rim of CyD, so that a deeper penetration of the xanthine ring within the cavity is hindered. We penetrated this ring more deeply at intervals of 0.01 nm and calculated the theoretical shifts of the CyD protons to find a better structure. Thus, we obtained structure **B** of the PB−α-CyD complex shown in Figure 9. In this structure, the side chain of PB is deformed to avoid a direct contact with the CyD. As the SS values in Table 2 show, structure **B** is better fit to the observed chemical shifts of the CyD protons than structure **A**.

Discussion

Amphiphilic compounds, such as many drugs, have the tendency of self-association and CyD inclusion. The effect of self-association of the guest molecule on CyD inclusion has been neglected in most investigations.[13] Although all aggregate species of PB must generally be taken into consideration, we neglected the species except for the dimer and micelles. The micelle of PB will be polydisperse in aqueous solutions above the cmc at 309.7 K as well as at 298 K in a 154 mmol dm^{-3} NaBr solution.[1] The difference between the cmc values of 18 and 10.5 mmol dm^{-3} under the two conditions will be ascribed mainly to the presence of NaBr. The dimerization constant of 20 dm^3 mol^{-1} in the present work is smaller than that of 31 dm^3 mol^{-1} in the presence of 154 mmol dm^{-3} NaBr.[1] This decrease in k_2 is also explicable in terms of reduced electric repulsion in the PB dimer, owing to NaBr. In the present work we are mainly concerned with the monomer concentration of PB at low PB concentrations. Under these conditions the monomer concentration of PB will be estimated rather accurately, even if the larger species other than the dimer of PB is neglected.

We considered two probable structures of the dimer of PB (Figure 5). The dimers of dyes and drugs having planar rings generally have rather parallel stacking structures.[5,21] Nitroxazepine and chlorpromazine both have tricyclic rings. The dimer of nitroxazepine is formed by intermolecular stacking of its middle ring B,[5] whereas that of chlorpromazine is formed by intermolecular stacking of its rings A and B.[21] For PB, however, the calculated chemical shifts for structure **B** is much closer to the observed values than those for structure **A** (Table 1).

The present 1:1 binding constant K_1 (61 dm^3 mol^{-1}) of PB and α-CyD is very close to those of 80 (surface tension method) and 90 (UV) dm^3 mol^{-1} in a 154 mmol dm^{-3} NaBr solution.[2] The present result implies some interpretation of 1:1 and 2:1 binding constants, K_1 and K_3, of PB with α-CyD. The second PB molecule binds to the 1:1 complex of PB and α-CyD anticooperatively ($K_1 = 230$ dm^3 $mol^{-1} > K_3 = 70$ dm^3 mol^{-1}).[2]

This anti-cooperative binding may be explained by two reasons. One of the reasons is a small dimerization constant of PB. This leads us to suggest that the second ligation of PB to α-CyD is less easy than the first ligation. The other reason is that the dimer structure of PB in the 2:1 complex would have a parallel stacking of the tricyclic ring of PB,[2] different from that of the solution structure: as the dimer, the solution structure will be more stable than the complex structure.

The structure of the 1:1 complex of PB and α-CyD (Figure 9) will be more hydrophilic than that of PB alone, so that the complex will be much less bitter than PB itself. This is consistent with our previous prediction.[2] Intermolecular NOE data for the PB and α-CyD system agree qualitatively with both the present structures (Figure 9) and are being analyzed quantitatively.[22]

References and Notes

(1) Funasaki, N.; Uemura, Y.; Hada, S.; Neya, S. *Langmuir* **1996**, *12*, 2214.

(2) Funasaki, N.; Uemura, Y.; Hada, S.; Neya, S. *J. Phys. Chem*. **1996**, *100*, 16298.

(3) Attwood, D.; Florence, A. T. *Surfactant Systems*; Chapman and Hall: London, 1983; Chapter 4.

(4) Funasaki, N. *Adv. Colloid Interface Sci*. **1993**, *43*, 87. Funasaki, N.; Hada, S.; Neya, S. *Trends Phys. Chem*. **1997**, *6*, 253.

(5) Attwood, D.; Waigh, R.; Blundell, R.; Bloor, D.; Thévand, A.; Boitard, E. Dubès, J.-B.; Tachoire, H. *Magn. Reson. Chem*. **1994**, *32*, 468.

(6) Marchettini, N.; Valensin, G.; Gaggelli, E. *Biophys. Chem*. **1990**, *36*, 65.

(7) Inoue, Y. *Ann. Rep. NMR Spectrosc*. **1993**, *27*, 60.

(8) Yamamoto, Y.; Onda, M.; Takahashi, Y.; Inoue, Y.; Chujou, R. *Carbohydr. Res*. **1988**, *182*, 41.

(9) Sherrod, M. In *Spectroscopic and Computational Studies of Supramolecular Systems*; Davies, J. E. D., Ed.; Kluwer Academic Press: Dordrecht, 1992; Chapter 7.

(10) Black, D. R.; Parker, C. G.; Scott Zimmerman, S.; Lee, M. L. *J. Comput. Chem*. **1996**, *17*, 931−939.

(11) Szejtli, J. *Cyclodextrin Technology*; Kluwer Academic Publishers: Dordrecht, 1988; Chapters 1 and 3.

(12) Bender, M. L.; Komiyama, M. *Cyclodextrin Chemistry*; Springer-Verlag: Berlin, 1978; Chapters 2 and 3.

(13) Connors, K. A. *Chem. Rev*. **1997**, *97*, 1325.

(14) Bovey, F. A. *Nuclear Magnetic Resonance Spectroscopy*; Academic Press: New York and London, 1969; Chapter 3 and Appendix C. Johnson, C. E., Jr.; Bovey, F. A. *J. Chem. Phys*. **1958**, *29*, 1012.

(15) Manor, P. C.; Saenger, W. *J. Am. Chem. Soc*. **1974**, *96*, 3630.

(16) Ford, B. L.; Wall, A. K.; Johnston, M. A.; Lea, A. R. *J. Assoc. Off. Anal. Chem*. **1984**, *67*, 934.

(17) Tomono, K.; Horioka, M.; Nagai, T. In *Minutes of the 6th International Symposium on Cyclodextrins*; Hedge, A. R., Ed.; Editions de Sainté: Paris, 1992; p 416.

(18) Aroney, M. J.; Hoskins, G. M.; Le Fevre, R. J. W. *J. Chem. Soc. B* **1969**, 980.

(19) Blackburn, A. C.; A. Dobson, A. J.; Gerkin, R. E. *Acta Crystallogr*. **1996**, *C52*, 1486. In crystals, xanthene 9-carboxylic acid forms the dimer, which is stabilized by hydrogen bond between the nearest carboxylic acid. A similar dimer will be formed in organic solutions. If it forms the dimer in aqueous solutions, its dimer will be stabilized by hydrophobic interaction between the xanthene rings of two xanthene 9-carboxylic acid molecules.

(20) Wood, D. J.; Hruska, F. E.; Saenger, W. *J. Am. Chem. Soc*. **1977**, *99*, 1735.

(21) Srivastava, S.; Phadke, R. S.; Govil, G. *Magn. Reson. Chem*. **1987**, *25*, 905.

(22) Hada, S.; Ishikawa, S.; Neya, S.; Funasaki, N. In manuscript preparation.